

AERODYNAMICS OF A GOLF BALL WITH GROOVES

Jooha Kim

School of Mechanical and Aerospace Engineering,
Seoul National University
Seoul 151-744, Korea
k-juha01@snu.ac.kr

Haecheon Choi

School of Mechanical and Aerospace Engineering,
Seoul National University
Seoul 151-744, Korea
choi@snu.ac.kr

ABSTRACT

In the present study, we investigate the aerodynamics of our newly designed golf ball that does not have dimples but grooves on its surface. We measure the drag and lift forces on the grooved ball in the ranges of real golf-ball velocity and spin rate, and compare them with those of smooth and dimpled balls. At zero spin, the drag coefficient on the grooved ball shows a rapid fall-off at a Reynolds number similar to that of a dimple ball and maintains nearly a constant value which is lower by 50 % than that of smooth ball. At non-zero spin, the lift-to-drag ratio of the grooved ball is higher than that of a dimpled ball by 5 - 20 % in the supercritical Reynolds number regime, but it is lower otherwise. With the measured drag and lift forces, the trajectories of the smooth, dimple and grooved balls are computed for the same initial condition. The flying distance of the grooved ball is larger than that of the smooth ball by 212 % and shorter by 6 % than that of the dimple ball, respectively.

INTRODUCTION

The characteristics of flow over a sphere are changed significantly by surface modification such as the surface roughness, trip wire, and dimples. Especially dimples reduce the drag on a sphere as much as 50% as compared to smooth surface and the reduced drag coefficient remains nearly constant over a range of Reynolds numbers. Choi et al. (2006) investigated the mechanism of drag reduction by dimples, and showed that turbulence is generated through the instability of shear layer separating from the edge of dimples. Smith et al. (2010) confirmed this mechanism from direct numerical simulation. Thus, triggering of the shear-layer instability before main separation is an important strategy for drag reduction. In this sense, it should be interesting to see if multiple grooves on the surface result in an aerodynamic characteristics similar to that of dimples.

In the present study, we devise a new golf ball that does not have dimples but grooves on the surface (Choi et al., 2008). To investigate the aerodynamic characteristics of the grooved ball, we measured the drag and lift forces on the grooved ball in the ranges of real-golf ball velocity and spin rate, and compare them with those of smooth ball and a golf ball with dimples.

EXPERIMENTAL SETUP AND PROCEDURE

Figure 1 shows the schematic diagram of the present experimental set-up, consisting of a sphere, motor, supporter, load cell, and an open-type wind tunnel. The cross-section of the wind tunnel after contraction is 600 mm × 600 mm and the turbulence intensity is lower than 0.5 % at the free-stream velocity of 10 m/s. A sphere of 150 mm diameter is made of acrylonitrile butadiene styrene (ABS) resin. A motor is installed inside the golf-ball model and rotates it about the vertical axis. The golf-ball model with motor is fixed to a supporter, which has an elliptic cross section. The upper part of the supporter is a pipe of 3 mm diameter. The lift and drag are measured by a load cell (BCL-3L) attached to the supporter. The rotational speed of the ball is measured by using a tachometer. We also measure the forces on a golf ball with dimples. Figure 2 shows the grooved ball used in our experiment. The depth and width of grooves considered are 0.8 and 10 mm, respectively. The grooves cover a golf ball almost uniformly.

The free-stream velocity U_0 varies from 5 to 27 m/s, corresponding to the Reynolds numbers, $Re = U_0 d / \nu = 0.5 \times 10^5 - 2.7 \times 10^5$, where d is the diameter of the sphere, ν is the kinematic viscosity. The rotational speed N varies from 0 (stationary) to 330 rpm, corresponding to the spin-rate ratios, $\alpha = \pi d N / 60 U_0 = 0 - 0.5$. These are within the ranges of real golf-ball velocity and spin rate. The measured forces are corrected by subtracting those of isolated supporter measured separately. The drag and the lift coefficients, C_D and C_L , are defined as

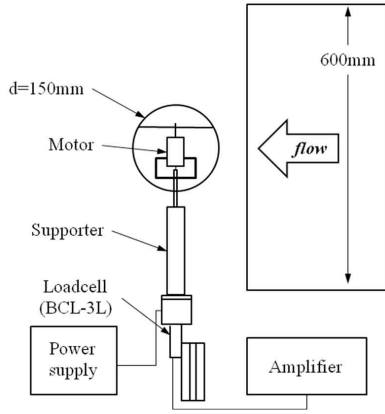


Figure 1. Experimental set-up

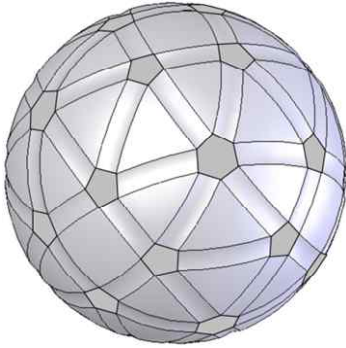


Figure 2. Grooved ball

$$C_D = \frac{D}{0.5\rho U_0^2 A}, C_L = \frac{L}{0.5\rho U_0^2 A} \quad (1)$$

where D is the drag, L is the lift, ρ is the density, and A ($= \pi d^2/4$) is the cross-sectional area of the sphere.

FORCE MEASUREMENT

Stationary Sphere

The drag is measured on a stationary smooth sphere and a golf ball with dimples. Figure 3 shows the drag coefficients of smooth, dimpled and grooved spheres, together with those of previous studies. The present drag coefficient of a smooth sphere shows good agreement with that of Achenbach (1972). Also, the present result of the dimple ball shows that the minimum drag coefficient is between the results of Bearman

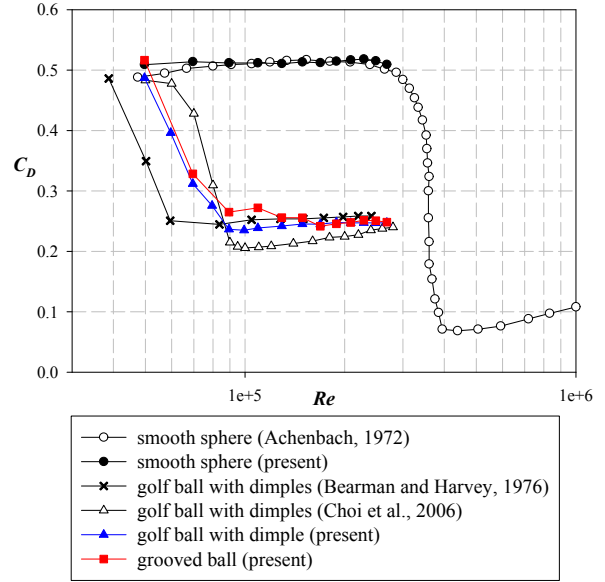


Figure 3. Drag coefficients of non-rotating smooth, dimpled and grooved balls

and Harvey (1976) and Choi et al. (2006). This is because the depth of present dimples ($k/d \approx 0.6 \times 10^{-2}$) is between those of Bearman and Harvey ($k/d = 0.9 \times 10^{-2}$) and Choi et al. ($k/d = 0.4 \times 10^{-2}$), where k is the depth of the dimples.

The drag coefficient of grooved ball shows a rapid fall-off at a Reynolds number similar to that of dimple ball, and its value is slightly higher than that of the present dimple ball near the critical Reynolds number range. However, the minimum drag coefficient is similar to that of the present dimple ball, showing 50 % drag reduction as compared to that of smooth ball.

Rotating Spheres

Drag Measurement The drags on dimple and grooved balls are measured at the free-stream velocities of 5 - 27 m/s and for three rotational speeds up to 330 rpm, which includes the range of real golf-ball velocity and spin rate. The variations of C_D with the free-stream velocity for dimple and grooved balls are shown in Figures 4 and 5, respectively, together with those of stationary dimple and grooved balls. The drag coefficient of dimple ball decreases with increasing free-stream velocity at same rotational speed, but it increases with increasing rotational speed when the Reynolds number is bigger than 0.5×10^5 (i.e. when the drag crisis starts) (Figure 4). The present result agrees well with that of Bearman and Harvey (1976).

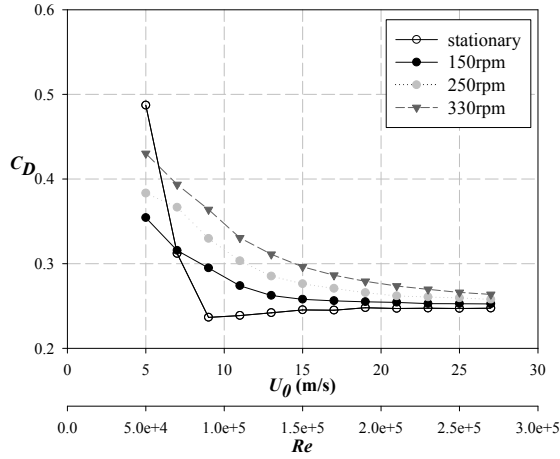


Figure 4. Variations of the drag coefficient for dimple ball with the free-stream velocity

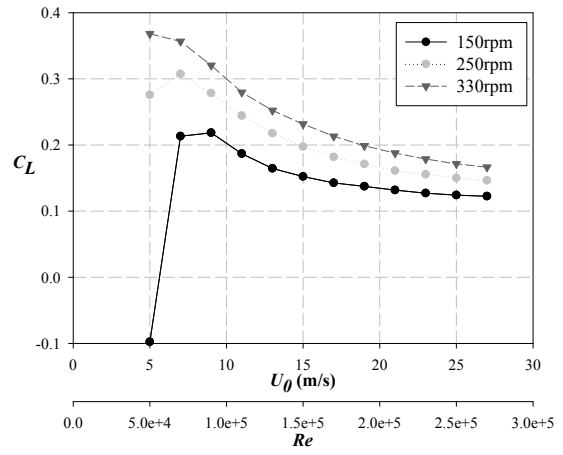


Figure 6. Variations of the lift coefficient for dimple ball with the free-stream velocity

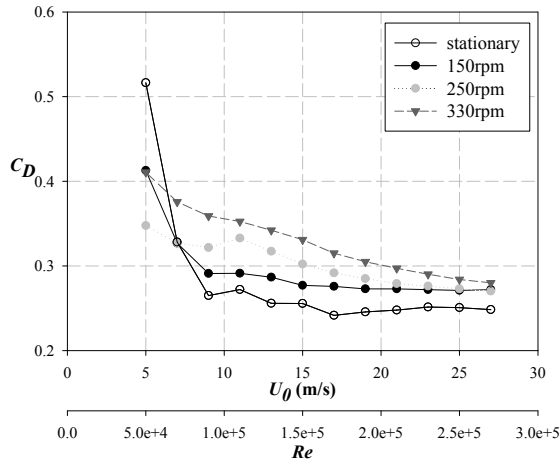


Figure 5. Variations of the drag coefficient for grooved ball with the free-stream velocity

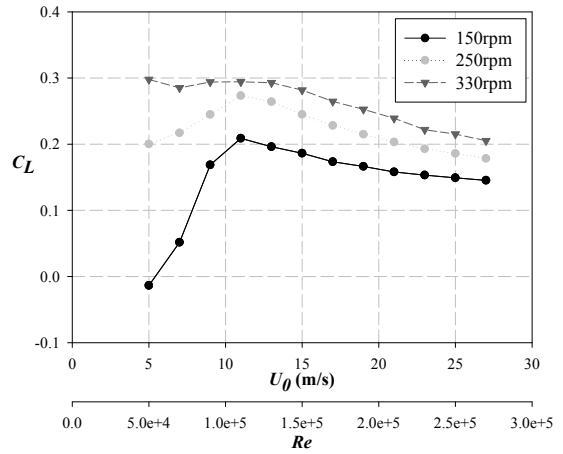


Figure 7. Variations of the lift coefficient for grooved ball with the free-stream velocity

On the other hand, the drag variation of grooved ball is similar to that of dimple ball when $Re > 0.7 \times 10^5$, but shows some complicated behaviour at sub-critical Reynolds numbers (Figure 5).

Lift Measurement The lift variations of dimple and grooved balls are shown in Figures 6 and 7, respectively. For both balls, the lift coefficient becomes bigger with higher rotation rate, and it decreases with increasing free-stream velocity after reaching its maximum value. The free-stream velocity showing maximum value of the lift coefficient

becomes smaller at higher rotation rate. Note that C_L becomes negative at $Re = 0.5 \times 10^5$ and $\alpha = 0.236$. This phenomenon is known as negative Magnus effect. The same negative lift was also observed in Bearman and Harvey (1976).

Lift-to-drag ratio The variations of lift-to-drag ratio (L/D) with the spin-rate ratio (α) for dimple and grooved balls are shown in Figure 8 for $Re = 1.1 \times 10^5 - 2.7 \times 10^5$, at which both dimple and grooved balls show supercritical behaviours. The drag and lift coefficients of grooved ball are also compared to those of dimple ball. It is shown that the drag coefficients of grooved ball are higher by 4 - 10 % than those

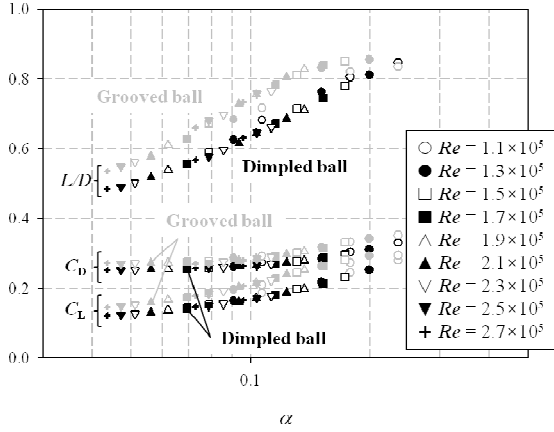


Figure 8. Variations of C_D , C_L and L/D with the spin-rate ratio (α) in the supercritical Reynolds number regime

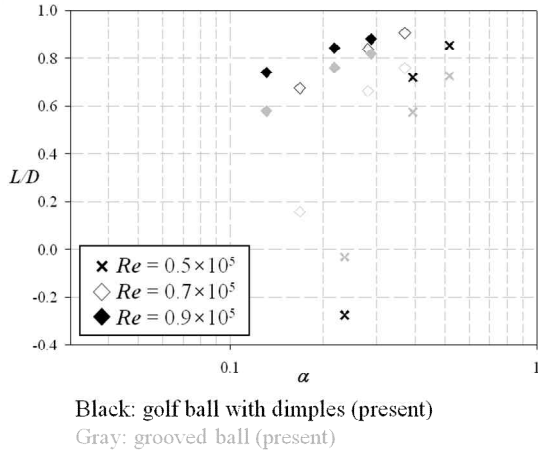


Figure 9. Variations of L/D with the spin-rate ratio (α) in the sub- and critical Reynolds number regimes

of dimple ball, but the lift coefficients of grooved ball are also higher by 10 - 27 % than those of dimple ball. As a result, the lift-to-drag ratios of grooved ball are higher by 5 - 20 % than those of dimple ball, implying that the aerodynamic performance of grooved ball is better than dimple ball in the ranges of Reynolds number and spin-rate ratio considered (i.e. in the super-critical flow regime).

On the other hand, at the sub- and critical Reynolds number regimes, the performance of grooved ball is not better than that of dimpled ball (Figure 9), showing lower overall lift-to-drag ratios of grooved ball than those of dimpled ball.

COMPUTATION OF TRAJECTORIES

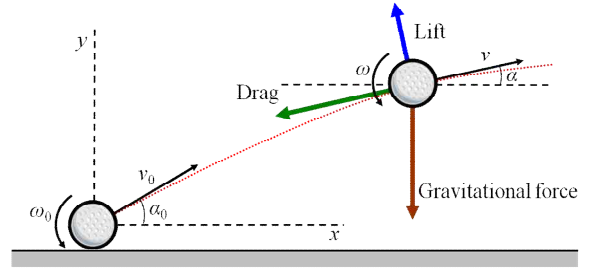


Figure 10. Computation of trajectories

Table 1. Initial conditions for a typical driver shot

v_0	α_0	ω_0
76 m/s	10°	314 rad/s

Computational Details

With the measured aerodynamic forces and initial conditions, it is possible to compute the complete trajectory for a golf ball drive. For the computation of trajectories, it is assumed that the golf ball satisfies a quasi-steady state at every instance. The drag and lift coefficients are obtained from interpolation of the present data. The equations of motion are

$$\frac{d^2x}{dt^2} = -\frac{\rho A}{2m} \left[\left(\frac{dx}{dt} \right)^2 + \left(\frac{dy}{dt} \right)^2 \right] (C_D \cos \alpha + C_L \sin \alpha) \quad (2)$$

$$\frac{d^2y}{dt^2} = \frac{\rho A}{2m} \left[\left(\frac{dx}{dt} \right)^2 + \left(\frac{dy}{dt} \right)^2 \right] (C_L \cos \alpha - C_D \sin \alpha) - g \quad (3)$$

where x and y are the position of the ball in the horizontal and vertical directions respectively, m is the mass of the ball, α is the inclination of the flight path to the horizontal and g is the acceleration due to gravity (Figure 10). The effect of spin decay during a flight is also considered using the exponential spin decay model proposed by Smits and Smith (1994) which takes the form of

$$\omega(t) = \omega_0 e^{-\frac{cv}{R}t} \quad (4)$$

where ω is the spin rate (rad/s), ω_0 is the initial spin rate, c is the experimental constant ($= 5 \times 10^{-5}$), v is the velocity and R is the radius of the ball. Initial conditions are determined on

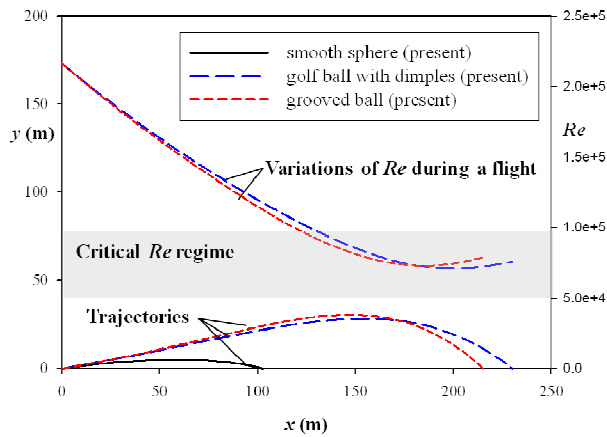


Figure 11. Trajectories and variations of the Reynolds number during the flights of dimpled and grooved balls

the basis of a typical driver shot (Table 1). The 4th-order Runge-Kutta (RK4) method is used for the computation with the time step size $\Delta t = 0.001$ s.

Trajectories

Figure 11 shows the trajectories of smooth, dimple and grooved balls at the same initial conditions. It is shown that the dimple ball flies 230 m and the flying distance is about 2.3 times farther than that of smooth ball. The flying distance of the grooved ball is 215 m, which is about 94 % that of dimple ball.

The variations of the Reynolds number during their flights are also shown in Figure 11 in the case of dimple and grooved balls. The Reynolds numbers of both dimple and grooved balls decrease as they fly and show slight increases at the ends due to the gravitational acceleration. In the beginning of the flight, the grooved ball flies higher than the dimple ball due to higher lift-to-drag ratios in the supercritical Reynolds number regime. However, the Reynolds number of the grooved ball decreases as the speed of the ball decreases and reaches the critical Reynolds number regime. The grooved ball rapidly descends due to lower lift-to-drag ratio in the critical Reynolds number regime, resulting in shorter flying distance than the dimple ball.

CONCLUSION

In this study, we evaluated the aerodynamic performance of our newly designed golf ball with grooves on its surface. At zero spin ($\alpha = 0$), the drag coefficient of grooved ball showed a rapid fall-off at a critical Reynolds number and maintained a minimum value which was 50 % lower than that on smooth ball, indicating that the multiple grooves on the surface

resulted in a similar aerodynamic characteristics to those of dimples at zero spin. At non-zero α , it was shown that in the supercritical Reynolds number regime the drag and lift coefficients of grooved ball were higher than those of dimple ball. As a result, the lift-to-drag ratio of grooved ball was higher by about 5 to 20 % than that of dimple ball. However, at the sub- and critical Reynolds number regimes, the performance of the grooved ball was not better than that of the dimpled ball, showing lower overall lift-to-drag ratios of the grooved ball than those of the dimpled ball.

With the measured aerodynamic forces, the trajectories of smooth, dimple and grooved balls were computed for same initial condition. The flying distance of grooved ball was larger by 212 % than that of the smooth ball but was 6 % shorter than that of dimple ball.

ACKNOWLEDGMENTS

This work is supported by the WCU, CRC, and Priority Research Center Programs through the NRF, MEST, Korea.

REFERENCES

- Achenbach, E., 1972, "Experiments on the flow past spheres at very high Reynolds numbers", *Journal of Fluid Mechanics*, Vol. 54, pp. 565-575.
- Bearman, P. W., and Harvey, J. K., 1976, "Golf ball aerodynamics", *Aeronautical Quarterly*, Vol. 27, pp. 112-122.
- Choi, H., Choi, J., and Son, K., 2008, "Golf ball", *Korean Patent*, 10-0803528.
- Choi, J., Jeon, W.-P., and Choi, H., 2006, "Mechanism of drag reduction by dimples on a sphere", *Physics of Fluids*, Vol. 18, 041702.
- Smith, C. E., Beratlis, N., Balaras, E., Squires, K., and Tsunoda, M., 2010, "Numerical investigation of the flow over a golf ball in the subcritical and supercritical regimes", *International Journal of Heat and Fluid Flow*, Vol. 31, pp. 262-273.
- Smits, A. J., and Smith, D. R., 1994, "A new aerodynamic model of a golf ball in flight", *Science and Golf II*, E&FN Spon, London, pp. 340-347.